The United Nations University

GEOTHERMAL TRAINING PROGRAMME
Orkustofnun, Grensásvegur 9,
IS-108 Reykjavík, Iceland

Reports 2003
Number 18

RESERVOIR PARAMETERS FOR WELL HE-5, HELLISHEIDI GEOTHERMAL FIELD, SW-ICELAND

Mahnaz Rezvani Khalil Abad
Renewable Energy Organization of Iran (SUNA)
Yadegar Emam Highway, Poonake Bakhtari Ave., Shahrake Ghods
P.O. Box 14155-6398, Tehran
IRAN
mare@iranenergy.org.ir

ABSTRACT

The Hellisheidi geothermal field is located within the Hengill high-temperature area in SW-Iceland. One of the wells in this area, HE-05, was directionally drilled. After completion of the well, HE-05 was tested for its pressure response to step injection. Data was analysed by using type curve matching and semi-log analysis. The skin factor for the well is estimated to be around -6, the transmissivity of surrounding formations around 2×10^{-4} m^3/Pas, and the formation storage about 6.4×10^{-8} m/Pa. Temperature and pressure profiles measured in the well during injection, warm-up and discharge were evaluated; and the formation temperature, initial pressure conditions in the vicinity of the well, and locations of possible aquifers in the well were determined. Two main and two minor feedzones are in the well. Formation temperature was evaluated, but the best result for formation temperature was obtained by using the last static temperature profile measured before flowing the well. A wellbore simulator was used to model the well during discharge and the results suggest two feedzones in the well. In addition, the wellbore model was used for prediction of pressure drop in each feedzone to estimate the flow conditions in the well. A production test showed that the capacity of this well for power generation is 3-4 MWe. The locations of the main feedzones, and the temperature in the lower part of the well agree with the current conceptual model for the Hellisheidi field.

1. INTRODUCTION

The vast geothermal system of the Hengill volcano in SW-Iceland is considered a potential resource for future electrical and heating needs for the city of Reykjavík and the surrounding communities. Reykjavík Energy is currently operating a 90 MW electric and 200 MW thermal unit in the Nesjavellir field in the northern part of the Hengill area (Gunnlaugsson, 2003). Nine deep production wells have been drilled to the south of Hengill volcano to explore the Hellisheidi area (Figure 1). Numerical reservoir modelling has been used as an integral part of field development and management strategy (Bödvarsson et al., 1990). A model for the Nesjavellir field, initially developed in 1986, has been recalibrated several times as more production and drilling data have become available. This effort is considered a success, as the model has consistently been able to forecast the field response to production. The favourable conditions observed

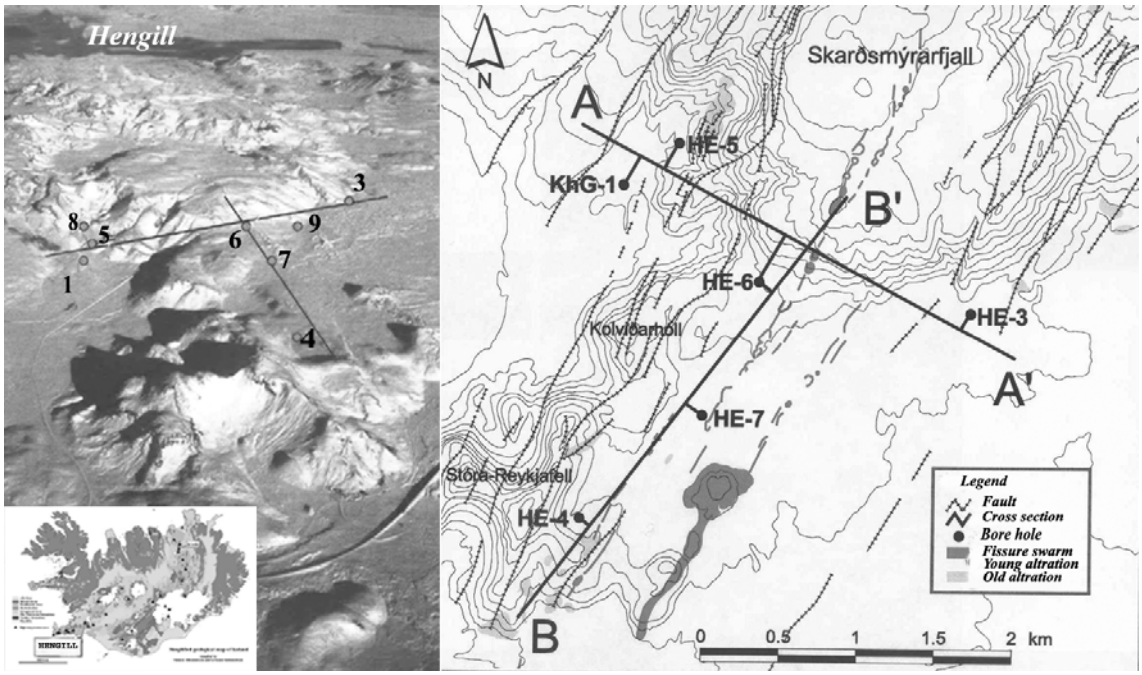

FIGURE 1: Location of the Hengill high-temperature area and boreholes in the Hellisheidi field (modified after Franzson and Kristjánsson, 2003)

in Nesjavellir awoke interest for the Hellisheidi field, to the south of the Hengill volcano. Reykjavík Energy expanded its land rights in the area and drilled exploration wells in Hellisheidi between 1994 and 2003. All these wells are productive, and are currently being thoroughly tested in order to characterize the Hellisheidi resource.

The purpose of this paper is to assess the reservoir characteristics of well HE-05 in Hellisheidi. Special emphasis is put on recording permeability and productivity indices for well HE-05. This data is considered highly valuable by providing permeability constraints for the numerical reservoir model that is currently under calibration. It is used to grid sub-elements, which are defined as feedzones or productive feedzones in geothermal wells. Other well information serves as a basis for defining the conceptual reservoir model in the area.

2. THE HENGILL AREA AND THE HELLISHEIDI GEOTHERMAL FIELD

The Hengill volcanic area, SW-Iceland, lies on the plate boundary between the North American and the European crustal plates. These plates are diverging at a relative speed of 2 cm/year. The rifting of the two plates has opened a north-northeast trending volcanic system of normal faults and frequent magma intrusions in SW-Iceland. The Hengill volcanic area and the high-temperature geothermal area is a product of this tectonic and volcanic activity. The Hengill area can in fact be divided into three distinct volcanic systems (Saemundsson et al., 1990). Each is composed of a central volcano and an intersecting swarm of fissures and hyaloclastite ridges. In the case of the youngest volcanic system, the Hengill system, it is characterized by a swarm of young crater rows and faults. The others are the Hrómundartindur and Hveragerdi volcanic systems to the east. They are both older and are gradually drifting out of the volcanic rift zone. Both are, however, probably underlain by solidifying magma chambers within the crust, which contribute to maintaining the associated high-temperature geothermal areas. The Hengill system probably contains magma in disconnected pockets that provides at least a part of the heat flow to the geothermal fields in this system. Geothermometers also indicate three separate heat sources, one for each volcanic system. The Hellisheidi geothermal field is a part of the Hengill system. It is to the south of Mt. Hengill, and covers an area of about 40 km^2. The active Hengill geothermal area is believed to have a natural discharge of 1000 MWt of thermal energy (Björnsson et al, 1986; Hersir et al., 1990; Saemundsson et al., 1990).

The Hengill area is located just north of a triple junction, where an oblique spreading axis and a major seismic zone meet. South of the Hengill central volcano, the axial rift zone in Iceland takes a westerly direction towards the tip of the Reykjanes peninsula where it continues as the Mid-Atlantic Ridge. On the other side, the volcanic rift continues with a northeast direction. To the east is the destructive South Iceland seismic zone. Presumably, tensional spreading is the most dominating factor in the tectonics of the Hengill area. Mt. Hengill symbolizes the central volcano and rises about 550 m above its surroundings, to an elevation of 800 m a.s.l. It is intersected by a major fissure swarm, that is over 50 km long, trending N30-35˚E and has a structure of nested grabens. Besides the main fissure swarm, there are some faults and eruptive fissures transecting the centre of Hengill in a NW-SE direction towards the Hveragerdi system, i.e. perpendicular to the main tectonic trend. The natural formation of Mt. Hengill is a table mountain or Tuya. Though the Hengill system is the only currently active volcanic system in the area, its predecessors, the Hrómundartindur and Hveragerdi systems, are still very active seismically and host lively geothermal reservoirs (Saemundsson et al., 1990; Hersir et al., 1990).

The main rock types in the Hengill area are interglacial lava flows and glacial hyaloclastites that are younger than 0.7 million years. Volcanic rocks of basaltic composition (of tholeiitic or olivine-tholeiitic type) cover a large amount of the surface. The hyaloclastite ridges in the northeast, north, and west part of the area are composed of basaltic pillow lava, breccia and tuffs and formed during the last glacial periods. Flat lying Postglacial basaltic lavas cover the central parts of Hellisheidi, including postglacial lavas erupted 5000 and 2000 years ago (Saemundsson et al., 1990).

Three production fields have been developed within the greater Hengill area. At Nesjavellir, northeast of Mt. Hengill, a 90 MWe and 200 MWt power plant is currently in operation. At Hellisheidi, a resource assessment is underway, and a new 120 MWe power plant scheduled for 2006. In Hveragerdi, the geothermal energy is utilized by the local community for heating and especially greenhouse growing.

3. WELL HE-05

Well HE-05 at Hellisheidi is a directional well sited in the Hellisheidi geothermal field, located at the coordinates: X = 364109.08, Y = 396154.31, Z = 307 m a.s.l. Figure 2 shows the design of the well. The direction of the well is towards the central part of the Hengill mountain and volcano. The assumptions in the conceptual model, and the accumulation of other evidence has shown that the central volcano is the place of the main upflow zone. Drilling of well HE-05 was focussed on that, and in such a way as to intersect nearby fractures. The result of each well add to the conceptual model of this area, which is in continuous development. The results of well test data for this area show the initial pressure condition in the reservoir and pressure distribution in the field. These data give the best information on depths to the main feedzones, and the location of upflow zones and lateral flow, data that can be used for numerical modelling, which is in progress for this field. It was planned to drill the well to a depth of about 2000 m, with the kick-off point at about 300 m with inclination from 2.5˚ / 300 m to an inclination of 35˚ in direction of 50˚±10˚. The actual direction of well HE-05 became 58˚, and the kick-off point is at 320 m depth. The drilling plan and casing programme are given in Table 1 (Jónsson et al., 2002).

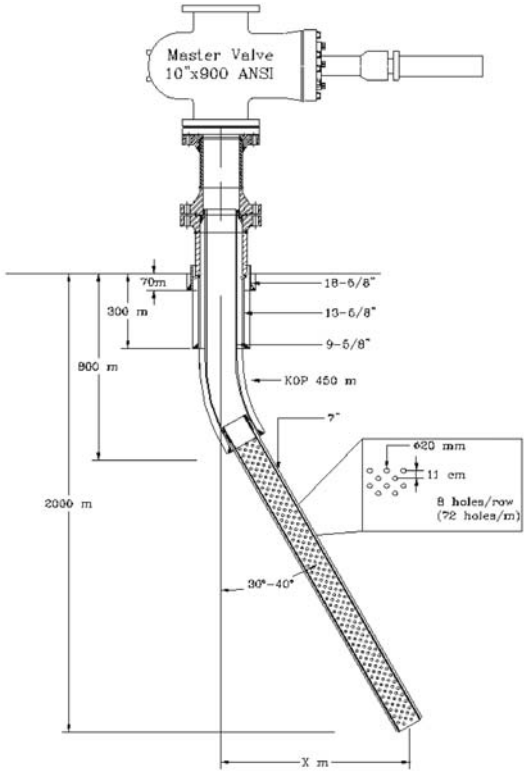

FIGURE 2: The casing design of well HE-05 (S. Thórhallsson, personal communication)

TABLE 1: Drilling plan, completion, and casing programme of well HE-05

Casing type and diameter (“)	Planned depth (m)	Drilled depth from cellar (m)	Casing depth from cellar (m)	True vertical depth (m)
Surface casing - 18 ⅝	75	90	90	90
Anchor casing - 13 ⅜	300	303	286	286
Production casing - 9 ⅝	800	795	792	746.5
Liner casing - 7	2000	1993	1917	1679.9

The true vertical depth of HE-5 compared to measured depth is presented in Table 2 and in Figure 3 along with the corresponding equation. This equation has been used to correct observed data in this report.

TABLE 2: True vertical depth and measured depth in well HE-05

Measured depth (m)	True vertical depth (m)
0	0
100	100
200	200
300	300
400	400.9
500	494.9
600	588.9
700	682.9
800	763
900	842
1000	921
1100	1000
1200	1079
1300	1158
1400	1230
1500	1319.7
1600	1390
1700	1470
1800	1554.9
1900	1609
1980	1679.9

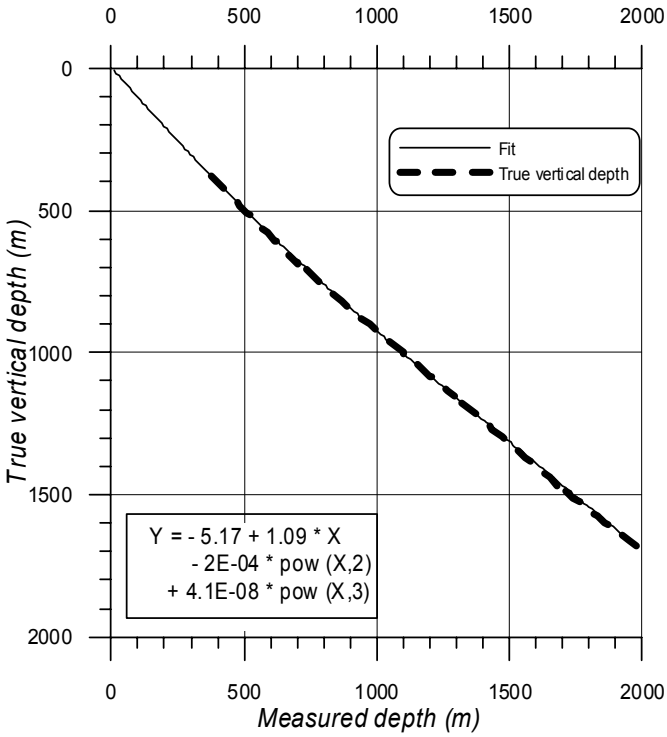

FIGURE 3: Graph showing true vertical depth of HE-5; also shown is an equation describing its relationship with measured depth

4. WELL TESTING

4.1 Theoretical background on well testing

During a well test, the response of a reservoir to changing production or injection (q) is monitored. Since the response is, to a greater or lesser degree, characteristic of the properties of the reservoir, it is possible in many cases to infer reservoir properties from the response. Well test interpretation is therefore an inverse problem in which model parameters are inferred by analyzing model response to given input.

In most well test cases, the reservoir response that is measured is the pressure response (p). Hence, in many cases well test analysis is synonymous with pressure transient analysis. The pressure transients are due to changes in production or injection of fluids; hence, the flow rate is treated as transient input and the pressure as transient output.

4.1.1 Pressure diffusion equation

The three governing laws that are used in deriving the pressure diffusion equation are the following:

a) Law of conservation of mass.

$$mass_{in} - mass_{out} = rate\ \ of\ \ change\ \ of\ \ mass\ \ accumulati\ on$$

b) Law of conservation of momentum, or Darcy's law (here in radial coordinates):

$$q = 2\pi h \frac{k}{\mu}\frac{\partial P}{\partial r} \tag{1}$$

where q = Volumetric flow rate per unit length (m^3/ms)
h = Reservoir thickness (m)
k = Formation permeability (m^2)
P = Reservoir pressure (Pa)
r = Radial distance (m)
μ = Dynamic viscosity of water (kg/ms)

c) Equation of state for water:

$$c = \frac{1}{\rho}\left(\frac{\partial \rho}{\partial P}\right)_T \tag{2}$$

where c = Compressibility of water (Pa^{-1})
ρ = Density of water (kg/m^3)
T = Temperature (˚C)

From Equations 1 and 2, the following radial pressure diffusion equation can be derived:

$$\frac{\partial}{\partial r}\left(\frac{r\partial P\,(r,t)}{\partial r}\right) = \frac{\mu\, c_t}{k}\left(\frac{\partial P(r,t)}{\partial t}\right) \tag{3}$$

where $P\,(r,\ t)$ = Reservoir pressure at distance r and time t (Pa)
c_t = Compressibility of wet reservoir formation (Pa^{-1})
t = Time (s)

The radial pressure diffusion equation is a partial differential equation that describes isothermal flow of fluid in porous media and how the pressure $P(r,\ t)$, diffuses through the reservoir. Initial and boundary conditions are required to solve for $P(r,t)$. For an infinite acting reservoir, the boundary conditions are:

a) Initial conditions:

$$P(r,t) = P_i \qquad for \quad t = 0, \quad r > 0 \tag{4}$$

where P_i = Initial reservoir pressure (Pa)

b) Inner and outer boundary conditions:

$$P(r,t) = P_i \quad r \to \infty \quad and \quad t > 0 \tag{5}$$

$$q = 2\pi r \frac{kh}{\mu}\frac{\partial P}{\partial r} \quad r \to 0 \quad and \quad t > 0 \tag{6}$$

The solution of the radial pressure diffusion equation, P(r,t), for the above initial time and boundary conditions is then:

$$P(r,t) = P_i + \frac{q\mu}{4\pi kh} E_i\left(-\frac{\mu c_t r^2}{4kt}\right) \tag{7}$$

E_i is the exponential integral function defined as:

$$E_i(-x) = -\int_x^{\infty} (\frac{e^{-u}}{u})du \quad with \quad x = \frac{\mu c_t r^2}{4kt}$$

For $x < 0.01$: $E_i(-x) \cong \gamma + \ln x$,

where γ = 0.5772 is the Euler's constant.

Therefore, if $t > 100\ \mu c_t r^2/4k$ and if one uses $\ln x = 2.303 \log x$, then the solution for the radial pressure diffusion equation can be simplified to:

$$P(r,t) = P_i + \frac{2.303q\mu}{4\pi kh}\left[\log\left(\frac{\mu c_t r^2}{4kt}\right) + \frac{\gamma}{2.303}\right] \tag{8}$$

This solution for the radial pressure diffusion equation is called the Theis solution or line source solution (Hjartarson, 2002). In deriving the Theis solution, the following assumptions are inherent:

1. The flow is considered isothermal and radial;
2. The reservoir is homogenous, isotropic, has infinite horizontal extent and uniform thickness;
3. The production well penetrates the entire formation thickness;
4. The formation is completely saturated with a single-phase fluid.

4.1.2 Semi-logarithmic well test analysis

The Theis solution can be written as:

$$P_i - P(r,t) = \frac{2.303q\mu}{4\pi kh}\left[\log\left(\frac{4k}{\mu c_t r^2}\right) - \frac{\gamma}{2.303}\right] + \frac{2.303q\mu}{4\pi kh}\log(t) \tag{9}$$

The above equation is in the form $\Delta P = A + m \log(t)$, which is a straight line with the slope m on a semi-log graph where:

$$\Delta P = P_i - P(r,t); \quad A = \frac{2.303q\mu}{4\mu kh}\left[\log\left(\frac{4k}{\mu c_t r^2}\right) - \frac{\gamma}{2.303}\right]; \ and \quad m = \frac{2.303q\mu}{4\pi kh}$$

The formation transmissivity, T, can be calculated from the slope of the semi-log straight line by

$$T = \frac{kh}{\mu} = \frac{2.303q}{4\pi m} \tag{10}$$

If the temperature is known, then the dynamic viscosity, μ, can be inferred from steam tables, thus, the permeability thickness, kh, may be calculated as follows:

$$kh = \frac{2.303q\mu}{4\pi m} \tag{11}$$

The formation storativity or storage coefficient, $S = c_t h$, is then obtained from the intercept with the ΔP-axis when the permeability thickness is known. The Theis solution can then be written as:

$$\frac{\Delta P}{m} = \left[\left[\log\left(\frac{4kh}{\mu}\right)\left(\frac{1}{S}\right)\left(\frac{t}{r^2}\right)\right] - \frac{\gamma}{2.303}\right] \tag{12}$$

$$\Rightarrow 10^{+\frac{\Delta P}{m}} = \left(\frac{kh}{\mu}\right)\left(\frac{1}{S}\right)\left(\frac{t}{r^2}\right)\left(4\times 10^{\frac{-\gamma}{2.303}}\right) \tag{13}$$

And the storativity can be obtained as:

$$S = 2.25\left(\frac{kh}{\mu}\right)\left(\frac{t}{r^2}\right)\times 10^{\frac{-\Delta P}{m}} \tag{14}$$

Since, the transmissivity, $T = kh / \mu$, then

$$S = 2.25T\left(\frac{t}{r^2}\right)\times 10^{\frac{-\Delta P}{m}} \tag{15}$$

Thus, a plot of ΔP vs. log t gives a semi-log straight line response for the infinite acting radial flow period of a well, and is referred to as a *semi-log analysis*. The semi-log analysis is based on the location and interpretation of the semi-log straight line response that represents the infinite acting radial flow behaviour of the well. However, as the wellbore has finite volume, it becomes necessary to determine the duration of the wellbore storage effect or the time at which the semi-log straight line begins.

The Theis solution for the constant rate drawdown test is based on the assumption that the down-hole production rate or injection rate changes instantaneously from zero to its constant value. However, due to the wellbore storage effect, the fluid flow out of the wellhead is not always the same as the flow from the reservoir into the well. That is, if a well is suddenly opened, the wellbore pressure will drop, causing expansion in boiling wells and water level depletion in non-boiling wells in the beginning. Similarly, if the well is suddenly shut in, the down-hole flow does not stop immediately but slowly tapers off. Several other factors can contribute to the wellbore storage effect but these above are the main factors. Therefore, it is important to find the beginning to the semi-log straight line correctly. The wellbore storage shows up as a unit slope straight line on a log-log plot of ΔP vs. t. As a working rule, there are about 1½ log cycles between the end of the unit slope straight line representing wellbore storage and the start of the purely infinite acting reservoir response. This 1½ log cycle rule provides a useful method of identifying the start of the semi-log straight line. The wellbore storage coefficient C (m^3/Pa) is defined as the volume, ΔV, of the fluid that the wellbore itself will produce due to a given pressure drop, ΔP, and is written as:

$$C = \frac{\Delta V}{\Delta P} \tag{16}$$

And for a well with free fluid level, the well bore storage coefficient is:

$$C = \frac{V_u}{\rho g} \tag{17}$$

where V_u = Wellbore volume per unit length (m^3/m);
ρ = Density (kg/m^3);
g = Gravitational acceleration (m/s^2).

But for a completely filled well, the fluid compression storage coefficient is given by:

$$C = c_f V_w \tag{18}$$

where c_f = Fluid compressibility;
V_w = Volume of wellbore (m^3).

Sometimes, there is a zone surrounding the well that is invaded by mud filtrate, cement, or cuttings during drilling and completion of the well, where the permeability is not the same as in the reservoir. This zone is called the skin zone. It produces an additional pressure drop, ΔP_s near the wellbore to the normal reservoir pressure change due to production, where s is the skin factor, which is dimensionless.

$$\Delta P_S = \frac{q\mu}{2\pi\, kh} \times s \tag{19}$$

where s = Skin factor (dimensionless)

If the skin factor is negative, the permeability of the skin zone is greater than the reservoir permeability indicating that the well may have been stimulated. On the other hand, if the permeability in the skin zone is less than reservoir permeability, the skin factor will be positive and the well is damaged. Skin factor can be used to calculate the radius of the skin zone if the permeability of the skin zone, k_s, and the permeability of the reservoir, k, are known:

$$s = \left(\frac{k}{k_s} - 1 \right) \ln \frac{r_s}{r_w} \tag{20}$$

Skin has a similar effect as changing the effective radius, r_{wa}, of the wellbore.

$$r_{wa} = r_w\, e^{-2s} \tag{21}$$

In pumping a well with skin, the total pressure change is given by:

$$\Delta P_t = \Delta P + \Delta P_s \qquad or \qquad \Delta P_t = P_i - P(r_w, t) + \Delta P_s \tag{22}$$

or

$$\Delta P_t = \frac{-2.303\, q\mu}{4\pi\, kh} \left[\log\left(\frac{\mu\, c_t r_w^{\,2}}{4kt} \right) + \frac{\gamma}{2.303} \right] + \frac{2s\, q\mu}{4\pi\, kh} \tag{23}$$

The above equation is used to deal with the additional pressure drop due to the skin effect during well testing. In semi-log analysis, the skin factor does not affect the evaluation of transmissivity but it does affect the evaluation of storativity as shown in the following equation:

$$c_t h\, e^{-2s} = 2.25 \left(\frac{kh}{\mu} \right) \left(\frac{t}{r_w^{\,2}} \right) \times 10^{\frac{-\Delta P}{m}} \tag{24}$$

In general, the steps involved in a semi-log analysis are:

a) Draw a log-log plot of ΔP versus Δt;
b) Determine the time at which the unit slope line representing wellbore storage ends;
c) Note the time of 1½ cycles after that point, which is the time at which the semi-log straight line can be expected to start;
d) Draw a semi-log plot of ΔP versus Δt;
e) Look for the straight line, starting at the suggested time point;
f) Estimate the transmissivity and storativity depending on the skin effect;
g) Estimate the skin factor.

4.1.3 Dimensionless variables and type curve well test analysis

Well test analysis often makes use of dimensionless variables in order to simplify the reservoir models by embodying the reservoir parameters, thereby generalizing the pressure equations and solutions. They have the advantage of providing model solutions that are independent of any particular unit system. Different reservoir models may have different boundary conditions giving rise to different solutions of the pressure diffusivity equation. Some of the solutions are mathematically complicated, and are therefore expressed as type curves that are dimensionless solutions associated with a specific reservoir model. Each appropriate reservoir model of a well test is found by plotting pressure transient data from a well test on a log-log graph and comparing it with various type curves. The following dimensionless variables are substituted in the pressure diffusion equation:

a) Dimensionless pressure, P_D

$$P_D = \frac{2\pi kh}{q\mu}(P_i - P(r,t)) \tag{25}$$

b) Dimensionless time, t_D

$$t_D = \frac{kt}{c_t \mu r^2} \tag{26}$$

c) Dimensionless radius or distance, r_D

$$r_D = \frac{r}{r_w} \tag{27}$$

Generally, the procedure for type curve analysis can be outlined as follows:

1. The data is plotted as log ΔP vs. log Δt on the same scale as that of the type curve.
2. The curves are then moved, one over the other, by keeping the vertical and horizontal grid lines parallel until the best match is found.
3. The best match is chosen and the pressure and time values are read from fixed points on both graphs, ΔP_M, P_{DM}, Δt_M, and t_{DM}.
4. For an infinite acting system, the transmissivity, T, is evaluated from:

$$T = \frac{kh}{\mu} = \frac{q}{2\pi}\frac{P_{DM}}{\Delta P_M} \tag{28}$$

5. And the storativity, S, is calculated as:

$$S = c_t h = \frac{kh}{\mu r_w^2}\frac{\Delta t_M}{t_{DM}} \tag{29}$$

4.2 Injection tests

In an injection test, fluid is injected into the well at a constant rate while the increase in downhole pressure is measured. It is conceptually similar to a drawdown test, except that the fluid flows into the well rather than out of it. It is used as a primary test to deduce geothermal properties and future productivity of a new well. Such test data from HE-5 was analyzed by using both semi-log and type curve matching methods.

4.2.1 Analysis of the HE-5 injection test

After completion of drilling, well HE-5 was initially injected with 49.3 l/s water for one hour to wash out the formation from invasion of filtrate and cuttings formed during drilling. This helps to alleviate the skin

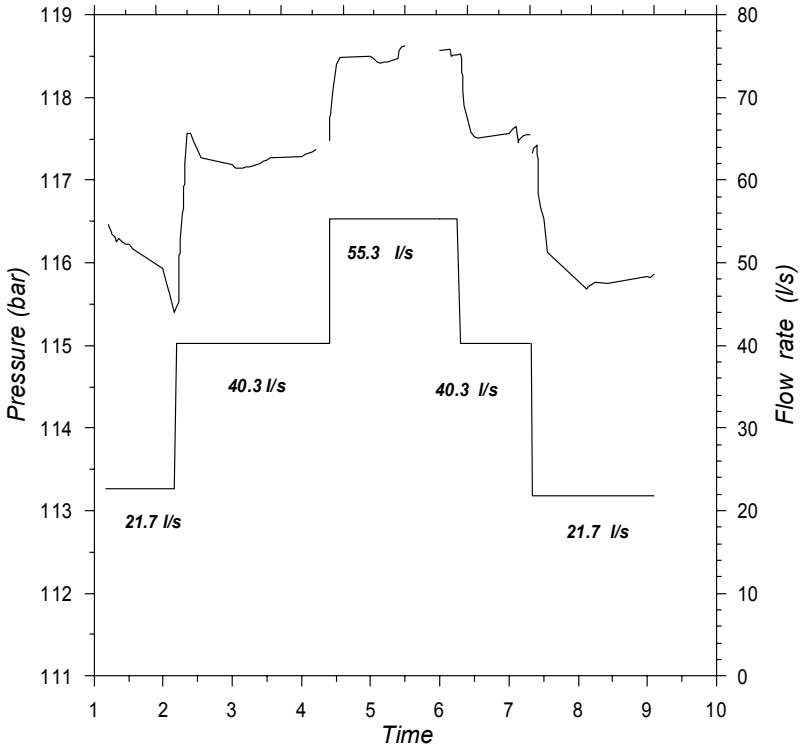

FIGURE 4: Pressure and flow variations during injection testing of HE-5

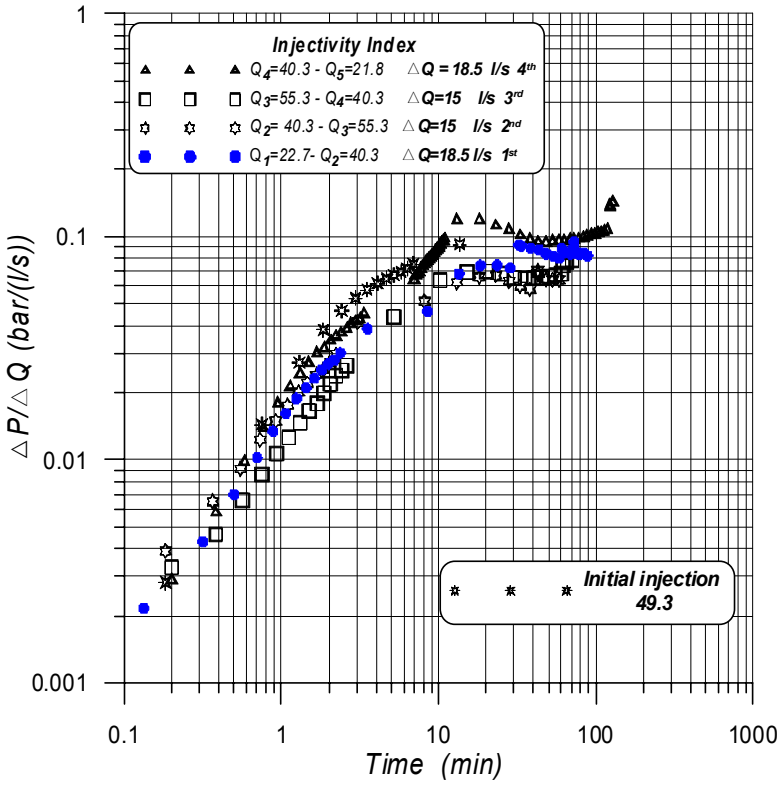

FIGURE 5: Unit pressure graph to find injectivity index for HE-5

effect problem, and achieve a stabilized flow rate before the injection test. Thereafter, injection flow rates were changed in steps of 40.3, 55.3, 40.3 and 21.8 l/s for the purpose of testing (Gudmundsson et al., 2002). A pressure gauge was located at a depth of 1700 m prior to the start of the injection test. Data collection started before a change was made in the injection flow rate, and it was saved before the rate was changed for the next step. The test was performed on 22-23 June 2002, the duration of each injection step being 196, 80, 78, and 140 minutes for the 40.3, 55.3, 40.3, and 21.8 l/s, injection rates, respectively. The downhole pressure was recorded by a pressure gauge at 1700 m depth during the injection test and the flow steps are shown in Figure 4.

The injectivity index reflects the success of the well. Injection of cold water can force the formation to accept more water through fractures and to create new fractures. A log-log graph of $\Delta P/\Delta Q$ (bar/l/s) vs. Δt was made for the steps (Figure 5). The values of the injectivity index, I_I, were obtained where the general behaviour of the curve was approaching stable condition on, or close to, a horizontal straight line at the end of each curve, i.e.:

$$I_I = \frac{\Delta Q}{\Delta P}$$

The Y value is the inverse of the injectivity index. A low value of Y indicates smaller pressure change due to changing of flow rate, and that the connection between the well and reservoir is good enough for quick pressure transition, and therefore the well has a good injectivity index. Moreover, it is possible to obtain some idea about transmissivity in the vicinity of the well. In this injection test, the first step was not successful. The injectivity index was around 15.5 (l/s/bar). It is greater than the value for the productivity index determined later, as can be seen in Section 4.2.3.

The injection test data were analysed by using a semi-log plot (Figure 6), and the type curve matching methods (Figure 7) to calculate transmissivity and formation storage for the well. In the semi-log plot of ΔP vs. Δt, care was taken in identifying the acting radial flow straight–line part of the plot, in order to avoid the wellbore storage effect in the early time of the plot. Then, the straight line was inferred, and its slope deduced for the calculation of transmissivity and formation storage. To use the type curve matching method, *P vs. t* was plotted and matched for the best fit between the data and the theoretical exponential integral solution for a single well in an infinite system. Wellbore storage and skin effects were included. The results of the semi-log analysis for transmissivity and formation storage are shown in Table 3 and results from type curve method are shown in Table 4.

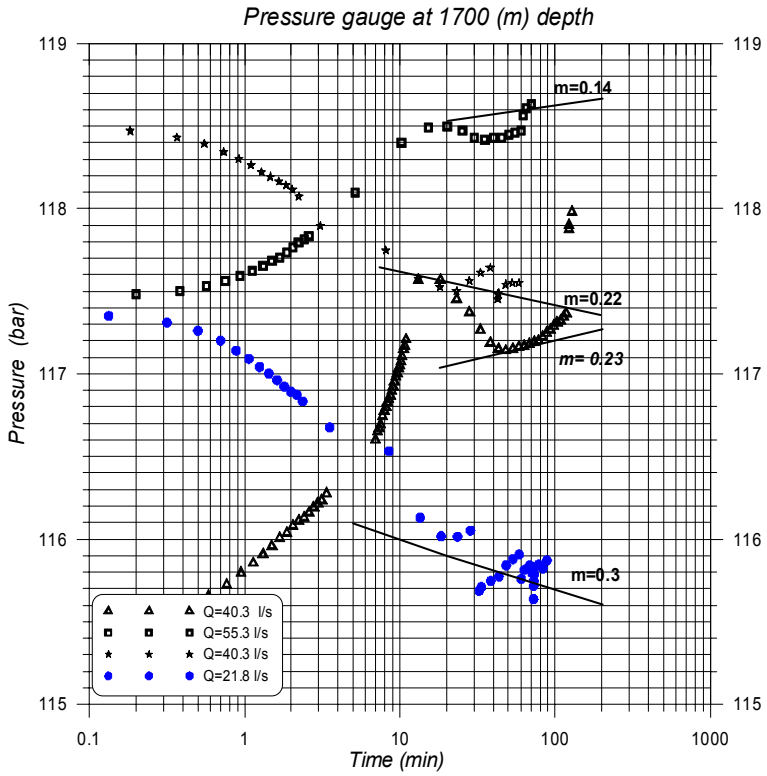

FIGURE 6: Plot of injection data for well HE-05 with interpretation based on semi-logarithmic analysis

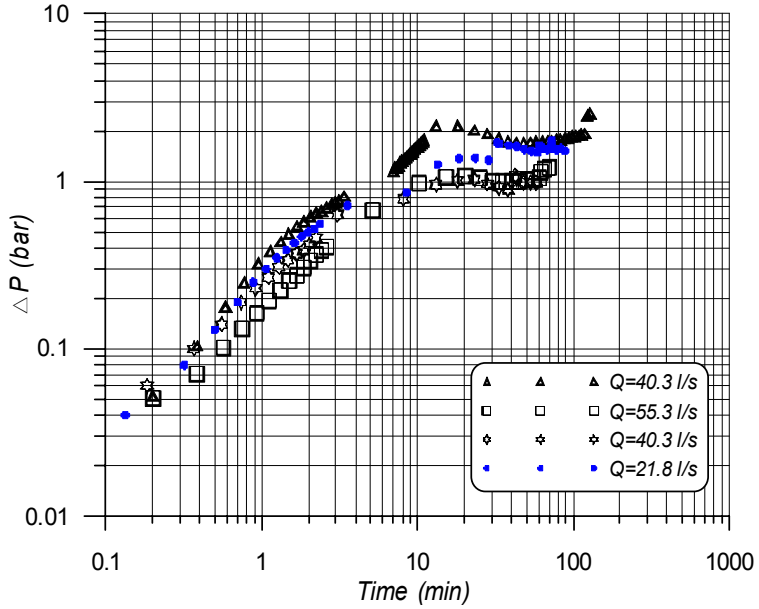

FIGURE 7: A log-log plot of injection data for well HE-05 used in the type curve matching analysis

TABLE 3: Results from semi-log analysis of injection data from HE-5

Injection flow rate (l/s)	**Transmissivity (m^3/Pas)**	**Formation storage skin effect included (m/Pa)**	**Semi-log slope (ΔP/1 log cycle)**
40.3	14.0×10^{-8}	2.83×10^{-9}	0.23
55.3	19.6×10^{-8}	7.66×10^{-9}	0.14
40.3	12.5×10^{-8}	116×10^{-8}	0.22
21.8	11.3×10^{-8}	27.2×10^{-8}	0.3

TABLE 4: Results of type curve matching, and matching with the Lokur program

Method	Injection rate (l/s)	Transmissivity (m^3/Pas)	Formation storage (m/Pa)	Wellbore storage	Skin
Type curve	40.3	29.4×10^{-8}	5.42×10^{-8}	10^5	10
	55.3	34.1×10^{-8}	5.2×10^{-8}	10^4	10
	40.3	15.9×10^{-8}	3.5×10^{-8}	10^4	0
	21.8	19.6×10^{-8}	48.6×10^{-8}	10^3	5
Lokur program	40.3	-	-	-	-
	55.3	1.91×10^{-7}	6.77×10^{-8}	7.21×10^3	1.7
	40.3	1.95×10^{-7}	6.28×10^{-8}	5.6×10^3	1.2
	21.8	1.57×10^{-7}	1.51×10^{-8}	3.7×10^4	-4.6

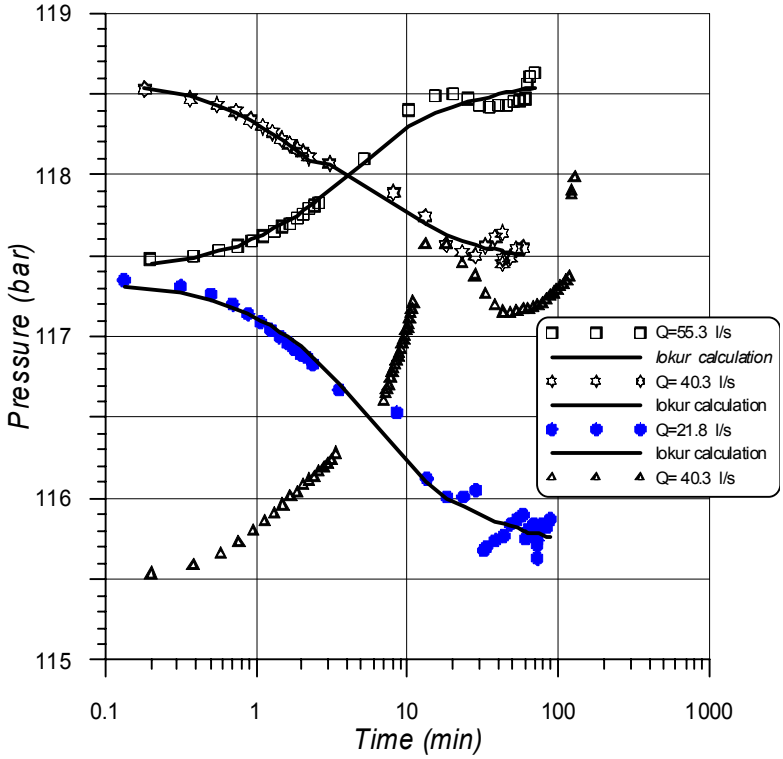

FIGURE 8: Semi-logarithmic plot of the match of Lokur program for the injection data from HE-5

The Lokur software was also used to calculate wellbore parameters for the injection steps. Lokur enables the use of different flow models to be tried to fit the raw data and calculate transmissivity, formation storage, wellbore storage, and skin effects. The data for the first step of the injection test was too noisy and is not included. The output plots of the Lokur program are shown in Figure 8 and the output parameters in Table 4. The parameters calculated for the four injection steps by the semi-log analysis are closer in their values than those of the type curve matching method. This could indicate that when both semi-log and type curve analyses are possible, the semi-log analysis is preferable. On the other hand, it is often difficult to select the best type curve as the difference between the curves is very small. It may be advantageous to have a rough estimate of some parameters beforehand, to select the most appropriate curve. The type curve analysis, in this case, is used to give some additional information. It shows that the early data, for less than thirty minutes, deviates from the later data which is not apparent in the semi-log analysis. The early data was influenced by wellbore storage and skin and other factors, and therefore the semi-log plot was refined to get the correct straight line. The correct straight line was identified by taking into consideration the general working rule that the wellbore storage effect shows up as a unit slope line at the beginning of the log-log plot and the correct straight line starts 1½ cycles after the unit slope line ends. As a result, the parameters calculated by using semi-log analysis were considered more reliable than those obtained from the type curve matching. The parameters calculated by using semi-log analysis were used as a first guess in the Lokur program. The analytical model used to fit the data was the infinite acting reservoir, including wellbore storage and skin present. Other choices of the program were the double porosity model with skin, fractured skin, and consideration of wellbore storage. Changing the model did not affect the outcome for the transmissivity and formation storage. The output parameters of the Lokur program were considered to be the most reliable of the three analysis methods, and represent the response of well HE-05 during the injection test.

4.2.2 Temperature and pressure logs of HE-05 during injection test

Information obtained from pressure and temperature logs during drilling and the injection tests form the basis for the first guesses for location of aquifers and flow patterns inside the well. Furthermore, determination of minimum reservoir temperature, and main loss or feed-zones obtained during drilling, are useful, in addition to the temperature and pressure logs, in blow-out risk evaluation, and in determining the physical state of the reservoir. The rate of change during circulation gives some idea about the flow rate and the time for warm-up, which are useful for protecting the instruments during logging and due to safety reasons. Cooling due to circulation and cold water pumping on the wellhead can be assessed, and bottom hole temperature determined. The main problem with downhole measurements during disturbed conditions is that temperature and pressure in the wellbore do not match those in the reservoir (Björnsson, 2002; Stefánsson and Steingrímsson, 1990).

Temperature and pressure logs were measured in HE-05 during drilling, during the injection test, and after completion. These data were analyzed to estimate the formation temperature and pressure, location of possible aquifers, and to simulate the flow pattern of the well. The pressure profiles measured during the injection test (Figure 9) gives the first measurements of the physical state of the reservoir. The change in slope in the graph at 780 m occurred because of gas accumulation in the casing shoe. The production casing starts at 800 m. Gas can make this kind of change in pressure, and it may be caused by a kind of boiling in the well. The pressure in the well was measured with a pressure gauge. The position of the gauge is shown in the legend in Figure 9. The first four profiles were taken during the initial injection while cleaning the well. Three profiles were taken during the 55.3, and 21.8 l/s injection test steps. The depth was corrected to true vertical depth in Figure 9. Evaluation of pressure profiles shows that there is no boiling in the reservoir and that the well is located in a liquid-dominated reservoir. More details can be seen by comparing the temperature and pressure profiles with the boiling point curve.

Downhole temperature profiles from HE-05 are shown in Figure 10. They include three runs during injection, four profiles during the warm-up

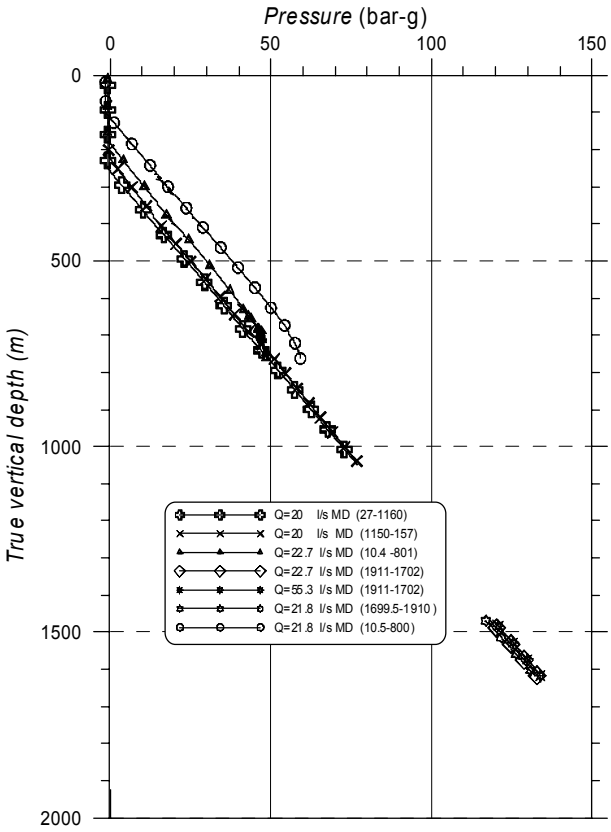

FIGURE 9: Downhole pressure during injection testing of HE-5 (evaluation of physical state in the reservoir)

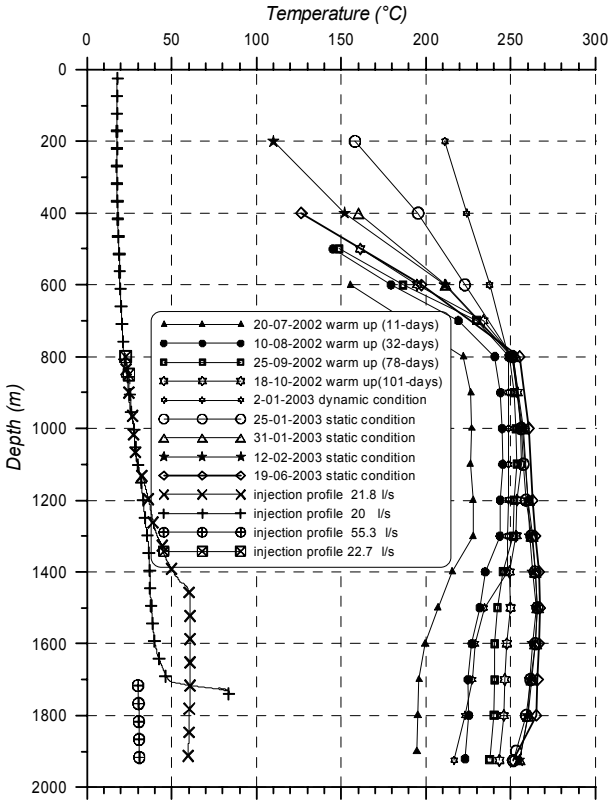

FIGURE 10: Injection, warm-up, and dynamic temperature profiles of HE-05

period, and five profiles while the well was flowing. The profiles were used to locate the main feedzone and aquifers in the well. According to the temperature profiles in Figure 10, a few aquifers are seen. The first one is at 800 m depth and the second at around 1400-1500 m depth, where a jump in the temperature gradient is observed during injection. According to this, the first guess about the location of the main feedzone in the well, is around 1400 m depth. During the injection test, temperature monitoring helped in locating the minor aquifers in the well. One minor aquifer is at 1200 m depth. At the bottom of the well, the temperature profiles show decreasing temperature indicating a colder aquifer there. The warm-up profiles down to 800 m, show that thermal conduction dominates the warm-up of the well. The casing blocks possible aquifers here. Below 800 m, the highest temperature in the well is around 270˚C at 1400 m depth. However, deeper in the well there is a reversal in the temperature profiles, which indicates colder water beneath the main feedzone, or that the higher temperature occurs due to a lateral flow in the area. During the heating-up period, the temperature change in the well at 1000 m depth was 35-40˚C. The aquifers deduced from the temperature profiles are summarized in Table 5.

TABLE 5: Possible aquifers (feedzones) in HE-05 deduced from the temperature profiles.

Aquifer location - T.V.D. (m)	Aquifer potential	Remarks
763	Minor	Injection temperature profile
1119	Minor	Injection temperature profile
1230	Main aquifer - controlling aquifer	Injection and warm-up temperature profiles
Bottom	Minor	Colder water manifested in warm-up and during production

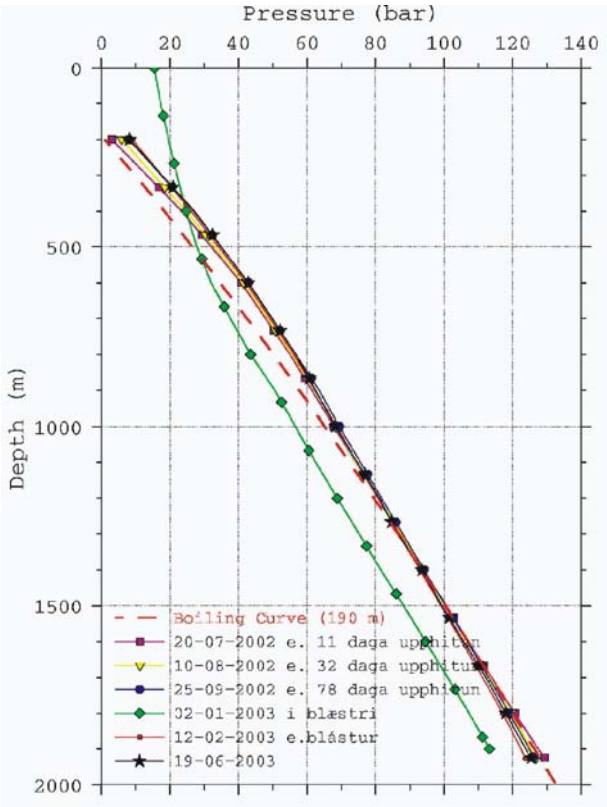

FIGURE 11: Injection, warm-up, and dynamic condition pressure profiles of HE-05 with boiling point pressure curve

4.2.3 Estimation of reservoir formation temperature

The boiling phase in the well can be evaluated from the boiling curve with depth. Water level in the well during the warm-up period was at around 200 m depth. If the boiling pressure curve starts at 200 m, it will pass through the pivot point, as can be seen in Figure 11. According to the pressure in the well, it is higher than the boiling point pressure. This means that no boiling could occur at the initial condition in the well. In the upper parts the pressure is higher than the boiling point curve, but at deeper levels it follows the boiling curve, while the temperature is lower than the corresponding boiling curve (Figure 12). During discharge, the liquid phase changes to a mixture of steam in the well at around 600 m measured depth. This is manifested in the pressure profile during discharge, which has been taken during dynamic conditions in the well. Similarly, the temperature profiles (Figure 12) were also below the boiling temperature curve. The initial temperature in the formation is below the boiling temperature.

During drilling, the well and the surrounding rocks are cooled. When drilling stops, it takes the some time to recover to its initial values. The temperature profiles and the boiling point curve are shown in Figure 12. Whether aquifers warm up more rapidly than the drier parts of the well depends on the well conditions. When flow is not present in the well, the aquifers usually warm up more slowly than the rest of the well, as aquifers experience more cooling during drilling. If on the other hand, fluid flow or boiling exists in the well, the reverse situation may easily occur. Therefore, warm up temperature profiles should be carefully analysed and associated with other information, especially to well conditions in order to evaluate the formation temperature of a well. Formation temperature serves as a basis for conceptual models, and is important in decision-making on well completion. The nearest point to the boiling point curve is located at 780 m.

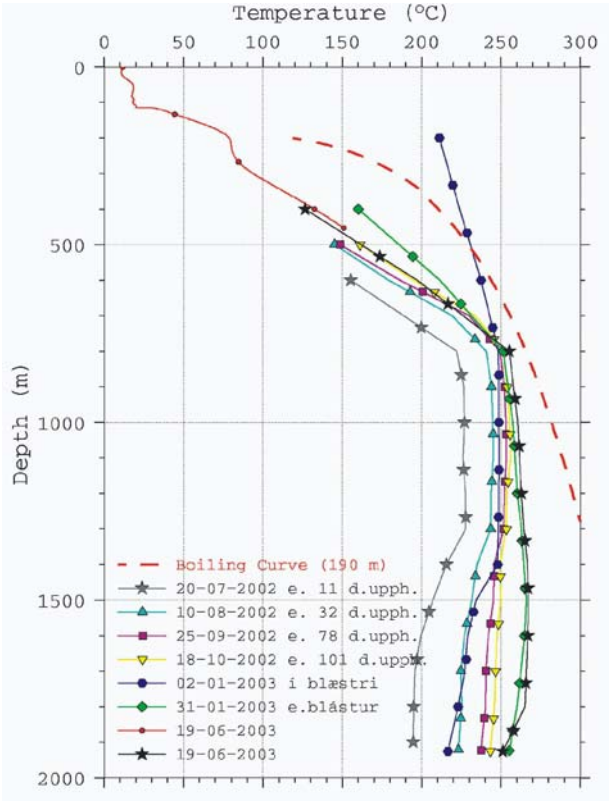

FIGURE 12: Injection, warm-up and dynamic condition temperature profiles of HE-05, and the boiling point temperature curve

The formation temperature in well HE-05 was estimated from the warm-up data at each depth to an infinite time with the Berghiti program in the ICEBOX software package (Arason et al, 2003). Berghiti uses a semi-analytical method to estimate formation temperature from time series of temperature logs taken during well warm-up. The program uses two methods, the Horner plot and the Albright methods, to estimate formation temperature. The Horner plot of temperature recovery is applied for longer warm-up histories, (weeks to months), and the Albright method for short time intervals, usually a few days.

The solution to the heat diffusion equation in radial coordinates is found by integrating the instantaneous response of a linear heat source over the cooling time duration, t_o, and is given by:

$$T(t) - T = \frac{q}{4\pi K} \ln \frac{t}{t - t_0} \qquad (30)$$

where t_0 = Cooling time;
q = Rate of heat removed from rock;
t = Time passed from drill bit intersection;
T_f = Formation temperature (˚C);
$T(t)$= Temperature at any time in the well (@˚C);
K = Thermal conductivity;
τ = $(t+t_0) / t_0$.

Thus, On a Horner plot, T vs. ln $((t+t_o) /t_o)$ is plotted, and the temperature at which the line crosses the $T(t)$ axis is taken to be the formation temperature. This method does not require that q and K are known, but q should be constant during drilling. The basic criterion for the technique is the straight line relationship that is between the maximum bottom hole temperature and ln τ, ($\tau = (t+t_o) / t_o$) and that $\lim_{t\to\infty} \ln \tau = 0$. Using this and the fact that the system must have stabilized after infinite time, the bottom hole temperature as a function of ln τ is plotted and then a straight line is inferred through the data. The formation temperature is obtained by extrapolating the straight line to ln $\tau = 0$ (Arason et al., 2003).

The Albright method assumes that for an arbitrary time interval much shorter than the total recovery time, the rate of temperature relaxation depends only on the difference between the borehole temperature and the formation temperature. If the whole logging time is represented as $I = [t_1, t_N]$, where N is the number of data points in the log, then for any time interval $i \in I$, $i = [t_a, t_b]$, there is $T_\infty{}^i$,c^i, and $T_0{}^i$ for $\forall\, t \in i$ that gives the best solution to the equation:

$$e^{-c^i t} = \frac{T_\infty{}^i - T^i(t)}{T_\infty{}^i - T^i{}_0} \tag{31}$$

where $T^i(t)$ = Temperature at time t, $t \in i$ (˚C);
T^i_∞ = Estimated equilibrium temperature for the time interval i (˚C);
$T_o{}^i$ = Temperature at the beginning of the time interval i (˚C);
c^i = Constant.

The formation temperature is determined assuming a linear dependence of c^i on $T^i{}_\infty$. Plotting c^i as a function of $T^i{}_\infty$, a straight line is inferred through the data and extrapolated for the X-axis interception to find the value of $T^i(t)$ as $t \to \infty$.

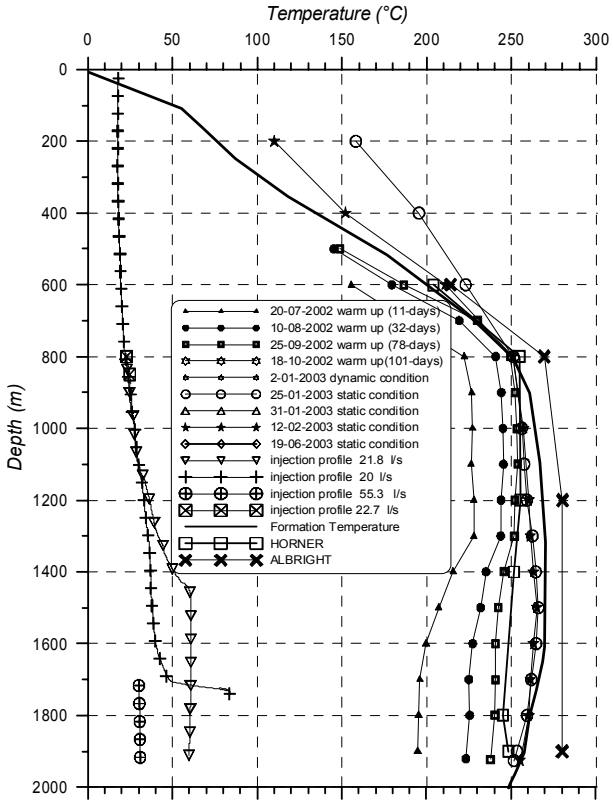

FIGURE 13: Formation temperature in HE-05 evaluated with Horner and Albright methods, along with the best result for formation temperature

The warm-up temperature data of HE-05 were analysed using both the Horner and Albright methods to determine the formation temperature. The obtained formation temperature was plotted with other temperature profiles for comparison in Figure 13. The warm-up temperature profiles got closer and closer together as the warm-up period increased, implying that the well was approaching thermal equilibrium after a short time, which is also reflected in the formation temperature evaluated using the Horner method. On the other hand, the Albright method estimates high temperatures compared to the dynamic profile that is the closest one to the situation in the formation. After a certain period of production and stability in the well, a realistic prediction for formation temperature can be made according to the last temperature log measured in the well. In this case, when a dynamic log from 19.06.2003 was taken, the temperature in the well had reached equilibrium, the temperature disturbances due to fluid flow and boiling had diminished, and the real temperature transferred from formation to the well bore.

Pressure logs, taken during warm-up and dynamic conditions from well HE-05, are shown in Figure 14. The pivot point is found at 1400 m measured depth with 94 bar pressure. True vertical depth correction is needed to correct the pressure values. True vertical depth is 1230 m and can be correlated with possible aquifers at the same depth (see Table 5). The pivot point indicates that the controlling feedzone of the well is located near this depth. The main feedzone in the well is located at or close to the pressure pivot point where pressure is assumed constant. Due to good hydraulic connection to the reservoir, the warm-up pressure profiles revolve around this pivot point (Björnsson, 2002; Stefánsson and Steingrímsson, 1980).

The productivity index, P_I, of the well can be determined by comparing the dynamic pressure condition with the pressure at static conditions in the well. The equation is:

$$P_I = \frac{\Delta Q}{\Delta P}$$

By using the total flow rate in dynamic conditions on 2-01-2003 which was 52 l/s (according to the profile in Figure 14), the pressure difference between static condition (pivot point - 94 bar), and the dynamic pressure at the same depth (82 bar), a productivity index of $P_I = 4.6$ is obtained. This is about three times lower than the injectivity index, I_I.

The formation temperature was used to calculate the pressure at true vertical depth in the formation. In the upper part, before the production casing is set, the pressure has to correspond with values obtained during drilling and information of circulation losses. In addition, for the deeper part below the production casing, the pressure was evaluated by the PREDYP program by giving the formation temperature and constant pressure at the pivot point (Arason et al., 2003). The depth of the pivot point was corrected to true vertical depth. A polynomial equation was used to simulate inclination of the well. Figure 15 shows the results of estimated temperature and pressure in the formation; it is also classified in Table 6.

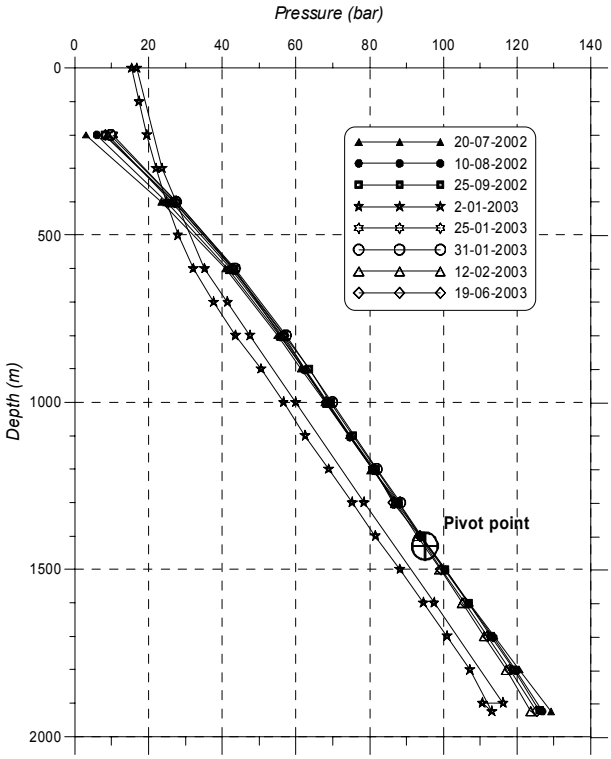

FIGURE 14: Pressure profiles during warm-up and dynamic conditions in well HE-05 with location of the pivot point

TABLE 6: Evaluated formation temperature and initial pressure of well HE-05

Measured depth (m)	Vertical depth (m)	Est. initial pressure (bar)	Est. form. temp. (°C)
0	0	0	3
100	100	0	35
200	200	20.58	70
300	300	30.87	100
400	400	41.16	133
500	494	50.83	170
600	588	57	200
700	682	66	225
800	763	74	250
900	842	63.72	252
1000	921	69.9	255
1100	1000	76.04	260
1200	1079	82.14	261
1300	1158	88.25	261
1400	1230	93.81	262
1500	1319.75	100.69	262
1600	1390	106.19	262
1700	1470	112.39	260
1800	1554.88	118.93	260
1900	1609	123.23	258
1980	1679.91	128.74	251

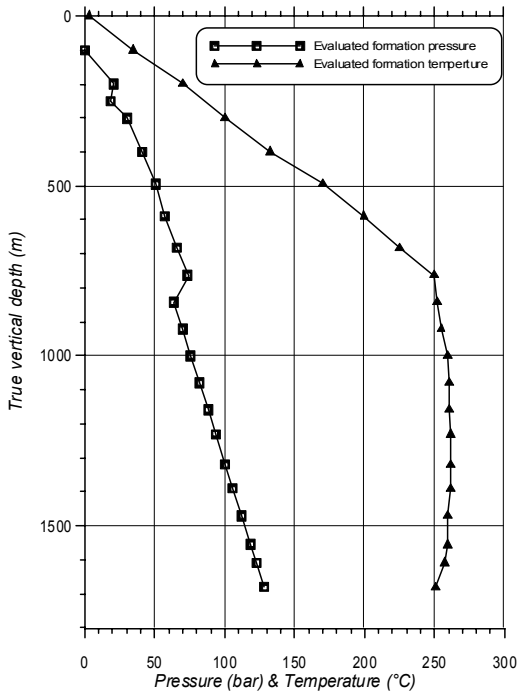

FIGURE 15: Evaluated formation temperature and initial pressure for well HE-05

4.3 Production test

A production test is conducted by flowing the well through an orifice to a silencer. Measurements are taken to evaluate the total flow rate, enthalpy, and chemical characteristics of the fluids. The output from a geothermal production well indicates how successful the exploration, siting and drilling of the well were. Furthermore, a production test is necessary for developers of geothermal projects to give an idea of the best utilization schemes for each production well, and how the reservoirs should be managed in the future. In order to analyse flow from wells, several measurements and flow tests are carried out. The most important flow parameters determined are:

1. Total mass flow;
2. Discharge enthalpy;
3. Non-condensable gas content and dissolved solids;
4. Well head pressure during discharge;
5. Pressure drop (drawdown) from the reservoir to the well during discharge;
6. Long-term variations in all the parameters that reflect the flow character of wells and the pressure drawdown in the reservoir – these are the fundamental data for predicting future response of the reservoir.

4.3.1 Theoretical background

The main parameters to be determined are the mass flow rate, the wellhead pressure, and the enthalpy of the produced fluid. An important assumption is normally made in determining enthalpy, that the flow in geothermal wells is isenthalpic; i.e. that any heat transfer due to thermal conduction between the wellbore and the surrounding formation is negligible. Thus, the enthalpy of the discharge is the sum of the enthalpy of the fluids entering at the feedzones. For high flow rates and long discharge time, this approximation is fairly accurate, but at low flow rates heat transfer (usually cooling) can be considerable as the fluid flows up the wellbore towards the wellhead (Steingrímsson, 2003).

A long-term production test was performed in well HE-05 in the year 2003 for 69 days. The method used to measure the flow rate and the enthalpy was the critical lip pressure and water flow rates method, which is the most common method of measuring two-phase discharge from geothermal wells. The method is based on a formula empirically deduced by Russel James (1970) for a large amount of steam or steam and water mixture flowing at sonic velocity through an open-ended pipe to the atmosphere. The absolute pressure at the extreme end of the pipe is then proportional to the mass flow rate and enthalpy. The formula that Russell James deduced empirically is:

$$Q = 1835000 \times A \frac{P_c^{0.96}}{H^{1.102}} \tag{32}$$

where Q = Mass flow (kg/s);
P_c = Critical pressure at the end of the lip pipe (bar-a);
A = Cross-section area of the lip pipe (m^2);
H = Fluid enthalpy (kJ/kg).

For two-phase applications, which is the case for well HE-05, the enthalpy of a two-phase mixture is used instead of steam enthalpy. Therefore, in order to quantify the discharge from the two-phase well HE-05, the following parameters were measured or calculated:

a) Total flow rate of steam and water, Q (kg/s);
b) Water flow rate, W (kg/s);
c) Steam flow rate, s (bar-a);
d) Lip pressure, P_c (bar-a);
e) Enthalpy, H (kJ/kg);
f) Mass ratio of steam to the total flow, X_s

The relationship of the total flow rate, Q, to the water flow rate, W, and the two-phase enthalpy, H, is given by:

$$Q = 1835000 \times A \frac{P_c^{0.96}}{H^{1.102}} \tag{33}$$

The enthalpy of the steam, H_s, and water, H_w, are taken from steam tables at atmospheric pressure, the pressure at which the two phases are separated in the silencer. Inserting these values for the specific enthalpy, the equation becomes:

$$Q = W \frac{H_S - H_w}{H_S - H_w} \tag{34}$$

During the production test, well HE-05 discharged through a lip pressure pipe into a silencer. Thereafter, wellhead pressure, critical pressure at the lip pipe, and the separated water at the weir box flowing from the silencer were measured. Thus, the enthalpy of the two-phase flow was given by:

$$\frac{1835000\, AP_C\, 0.96}{H^{1.102}} = W \frac{2256}{2676 - H} \tag{35}$$

The enthalpy H is the only unknown variable in the above equation, and is determined by iteration of the equation. After the enthalpy is determined, the total flow rate is calculated. Measured and calculated values from the production test are given in Table 7.

TABLE 7: Measured and calculated parameters of the production test in well HE-05

Date	WHP (bar)	Pc (bar)	Water height in weir box (mm)	Water flow (kg/s)	Total flow (kg/s)	Enthalpy (kJ/kg	High-pressure steam (kg/s)
07-Nov-2002	11.72	1.42	25.84	45.9	58.8	804	1.2
15-Nov-2002	12.15	1.48	20.49	25.9	41.3	1149	7.3
25-Nov-2002	12.85	1.56	23.38	35.8	52.3	970	4.9
30-Nov-2002	13.18	1.62	22.66	33.2	50.8	1030	6.1
05-Dec-2002	13.49	1.7	25.39	44	63.0	883	3.3
10-Dec-2002	13.77	1.68	22.77	33.5	52.3	1035	6.2
25-Dec-2002	14.67	1.89	24.3	39.4	62.0	983	5.8
30-Dec-2002	14.87	1.93	25.24	43.3	66.8	936	4.8
03-Jan-2003	15.02	1.93	22.41	32.3	55.3	1110	8.0
07-Jan-2003	15.16	1.94	22.14	31.3	54.4	1132	8.4
09-Jan-2003	15.19	1.92	24.61	40.7	63.9	969	5.5
12-Jan-2003	15.29	1.95	22.45	32.4	55.7	1113	8.1

4.3.2 Flow history of well HE-05

The flow history of the well for the 69 days of flow testing is shown in Figure 16. Production test data values considered for the graph were obtained at 12:00 am for each day. According to the value of high-pressure steam separation at 10 bar (see Table 7 and Figure 16), it shows that the value of steam is around 8 (kg/s). Thus, 3-4 MWe power generation is the initial guess for power generation capacity of this well.

4.3.3 Analysis of dynamic temperature and pressure profiles using the HOLA wellbore simulator

During the production period, total flow rate, amount of water flow, and wellhead pressure were monitored and the enthalpy determined. The wellbore simulator HOLA was used to find the downhole

conditions that fulfilled a required wellhead pressure. Reservoir pressure and pressures in the feedzones after the production period were available. The simulator HOLA reproduces the measured flowing temperature and pressure profiles in a flowing well, and determines the relative contribution of each feedzone for given discharge conditions (Arason et al., 2003). The flow within the well is assumed to be in steady state at all times. The simulator can handle both single- and two-phase flow in vertical pipes. The measured temperature and pressure has been corrected to true vertical depth for the well. The governing equations that describe the steady-state energy, mass, and momentum flow in a vertical pipe are given in the user's guide (Björnsson et al., 1993).

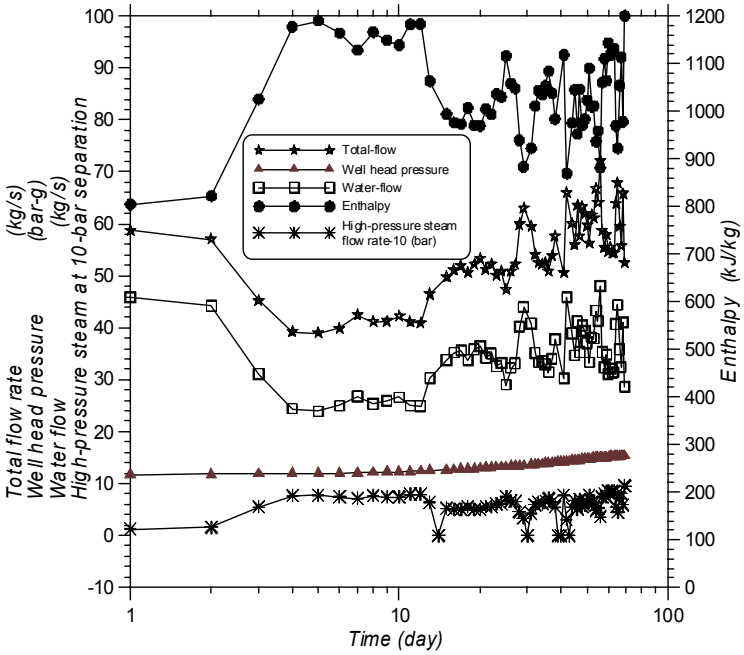

FIGURE 16: Flow history for production test of well HE-05

One of the last measured dynamic profiles from well HE-05 was simulated by varying the number of feedzones, enthalpy at feedzones, and flow contribution. Wellhead pressure, enthalpy, and total flow obtained during discharge were the values used to compare the results with. The outcome has to simulate and match measured temperature and pressure profiles, to get the best fit. In this case, the best fit is found for two feedzones and wellhead enthalpy of 1084 kJ/kg. The two feedzones are found at 1000 m vertical depth (1100 m measured depth) and at the bottom of the last section of the well (required for program), corresponding to the pivot point, 1230 m vertical depth (1400 m measured depth). The program was executed with depth increasing in 25 m steps, from wellhead down to 1250 m. The simulated results show that the fluid in the wellbore changes phase from single phase to steam and water mixture around the casing shoe. The flashing zone is located at 760 m vertical depth. The simulated dynamic wellbore parameters are given in Table 8, and the simulated profiles are shown in Figure 17.

TABLE 8: Simulated dynamic wellbore parameters using HOLA program

Depth (m)	Press. (bar-a)	Temp. (°C)	Dryness (%)	*Hw* (kJ/kg)	*Hs* (kJ/kg)	*Ht* (kJ/kg)	*Vw* (m/s)	*Vs* (m/s)	*Dw* (kg/m^3)	*Ds* (kg/m^3)	*Rad* (mm)	Reg
0	16.4	202.7	11.4	865	2793	1085	15.4	21.0	862	8.3	110	Sl
100	18.8	209.1	10.1	894	2796	1087	12.4	16.8	854	9.4	110	Sl
200	20.9	214.5	9.1	918	2798	1089	10.4	13.9	847	10.5	110	Sl
300	23.1	219.7	8	942	2800	1090	8.63	11.6	841	11.6	110	Sl
400	25.4	224.9	6.8	966	2801	1092	7.12	9.47	834	12.7	110	Sl
500	28.1	230.3	5.6	992	2802	1093	5.74	7.59	827	14.1	110	Sl
600	31.4	236.3	4.2	1020	2802	1095	4.42	5.81	819	15.7	110	Sl
700	35.7	243.6	2.4	1055	2802	1096	3.07	4	808	17.9	110	Sl
800	42.9	252.5	0	1098	0	1098	3.28	0	796	0	80	Tp
900	51.7	252.7	0	1099	0	1099	3.28	0	796	0	80	Tp
1000	60.5	253	0	1100	0	1100	3.28	0	797	0	80	Tp
1000	60.5	258.5	0	1127	0	1127	2.16	0	788	0	80	Tp
1100	68.6	258.7	0	1128	0	1128	2.16	0	789	0	80	Tp
1200	76.8	259	0	1129	0	1129	2.15	0	789	0	80	Tp

Sl = Single phase; Tp = Two phase

The HOLA wellbore simulator results can be used to predict the power generation and the capacity of the well during discharge. The obtained model can also predict the future discharge situation according to pressure drop in the reservoir, cooling in the well, or change in enthalpy or pressure in the feedzones.

Pressure in the reservoir for the best model is 95 bar-a. For prediction, the pressure at the deeper feedzone was lowered by 5 bar. According to estimation during the injection test and warm-up period, the deeper feedzone has a higher productivity index and is governing the pressure situation in the well. The productivity index for the bottom-hole feedzone is three times higher than for the minor one. Moreover, the higher temperature and higher enthalpy is affected by this feedzone in the well. The well is a good production well. According to the Hola model at 10 bar-a well head pressure, this well could supply 5 kg/s high-pressure steam. This means 2 MW electrical power generation is expected from this well. Also, the production history shows that the average value for high-pressure steam is more than 5 kg/s. The best model of HOLA is shown in Figure 18. The black point is a measured at the wellhead.

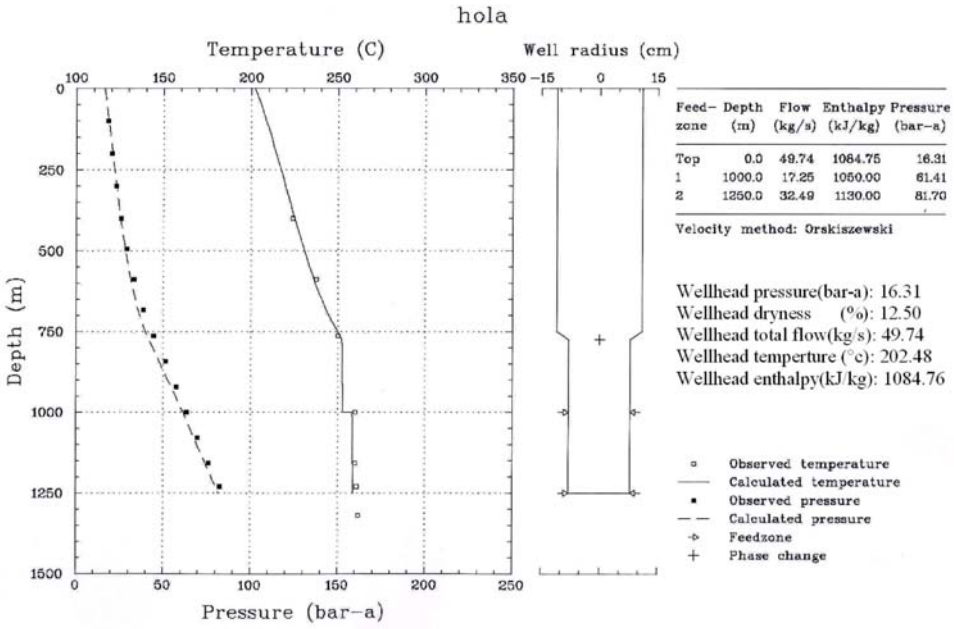

FIGURE 17: Output of HOLA wellbore simulator being used on well HE-05

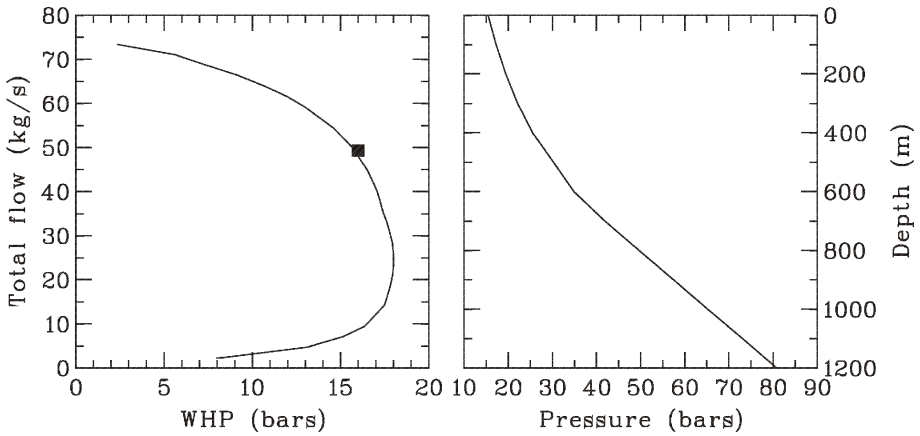

FIGURE 18: Hola best model for simulating the wellhead observation data for HE-5

In Figure 19, HOLA was used to predict the pressure drop at the main feedzone from 95 bar-a to 90 bar-a. The main feedzone controlling the discharge of the well with 5 bar pressure drop changes the behaviour of the curve, as can be seen in Figure 19. On the other hand, if the pressure drop occurs at the feedzone

at 1000 m depth, the change in the behaviour of the curve is actually so small that it does not change the capacity of the well very much, as can be seen in Figure 20.

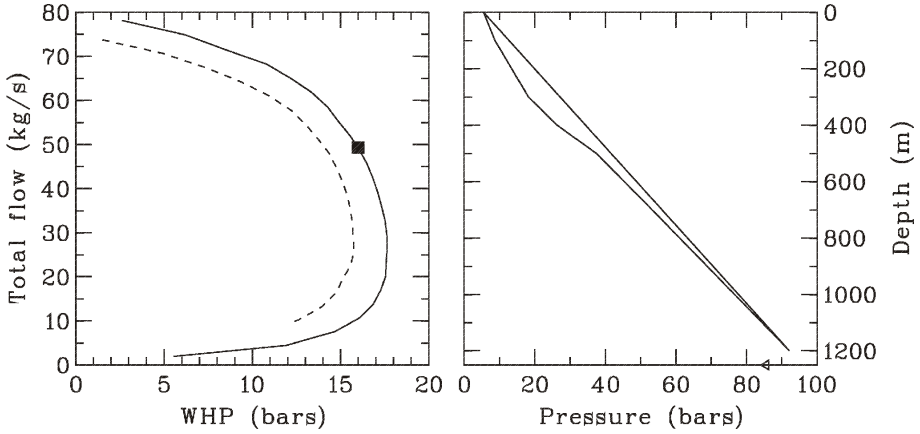

FIGURE 19: HOLA prediction for 5 bar pressure drop in the main feedzone of HE-5

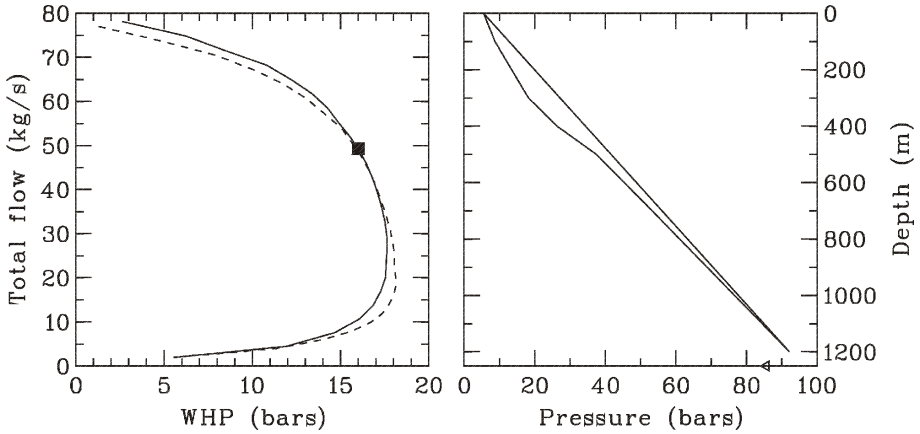

FIGURE 20: HOLA prediction for 7 bar pressure drop in the feedzone located at 1000 m depth in HE-5

4.4 Recovery and pressure build up

The well was shut in after 69 days of production as already mentioned. Pressure or recovery build-up measurements were done following this. The data have been plotted as Δp vs. Δt using a log-log graph. In addition, data have been plotted for semi-log analysis with Horner time. A production time t_p is used that corresponds to the final discharge rate q. This provides the means to generate the pressure response during a build-up test, using the simple constant rate solutions generated for drawdown tests as shown in the following equation:

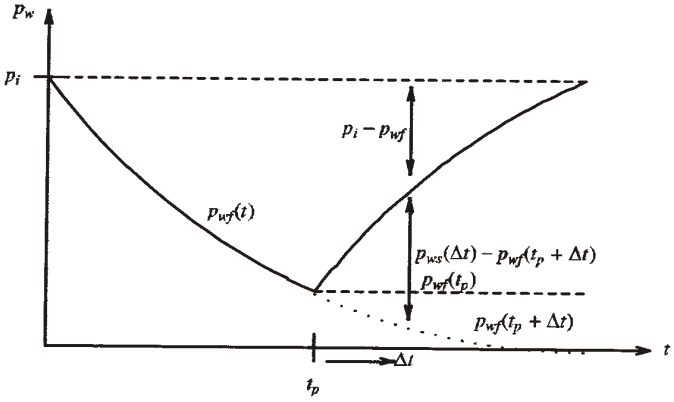

FIGURE 21: Illustration of the definition of Horner time (Horne, 1995)

$$p_D(t_D) = p_D(t_{p_D} + \Delta t_D) - p_D(\Delta t_D) \tag{36}$$

This is illustrated in Figure 21, and is true regardless of the reservoir model used.

The reservoir behaviour is expected to dominate true recovery after a shut-in time Δt of about 300 minutes. This would correspond to a Horner time of $(t_p + \Delta t) / \Delta t = (69 \times 24 \times 60 + 300) / 300 = 332.3$. Plotting a Horner plot as in Figure 22, the Horner straight line is seen to start at around this point. The slope of the Horner straight line is 0.18 (bar/log cycle). Based on the slope of the straight line and the flow rate before shut-in, the transmissivity for the well can be estimated. As the last total flow rate from the well was 43.7 kg/s, transmissivity, T, and storativity, S, are estimated:

$$T = \frac{2.303 \times q}{4 \pi m} \qquad \text{or} \qquad T = 2.303 \times 43.7) / 4\,\pi \times 0.18 \times 10^5 = 4.44 \times 10^{-6}\ \text{m}^3 / \text{Pa s}$$

and

$$S = 2.25 \left(\frac{t}{r_w^{\,2}} \right) \left(\frac{kh}{\mu} \right) 10^{-\frac{\Delta p}{m}}$$

where Δp = 86.5 - 84.4 = 2 bar
$(\Delta t + t_p) / \Delta t$ = 1000
Δt = Actual time t = 99.45 s
P_i = 86.85 bar-g

Hence $S = 2.25\ (99.45 / 0.0121) \times 4.44 \times 10^{-6} \times 10^{-2/0.18} = 6.35 \times 10^{-13}$

Average undisturbed reservoir pressure P_i, can be obtained from the point at which the extension of the Horner straight line meets the axis $(t_p + \Delta t) / \Delta t = 1$, as in Figure 22. This point is sometimes known as the Horner extrapolated pressure or the Horner false pressure. The Horner plot result may also be used to estimate the skin factor, since the skin factor is dimensionless and represents a near wellbore pressure drop:

$$\frac{\textit{Formation storage with skin effect included}}{\textit{formation storage}} = \frac{c_t h e^{-2s}}{c_t h} \tag{37}$$

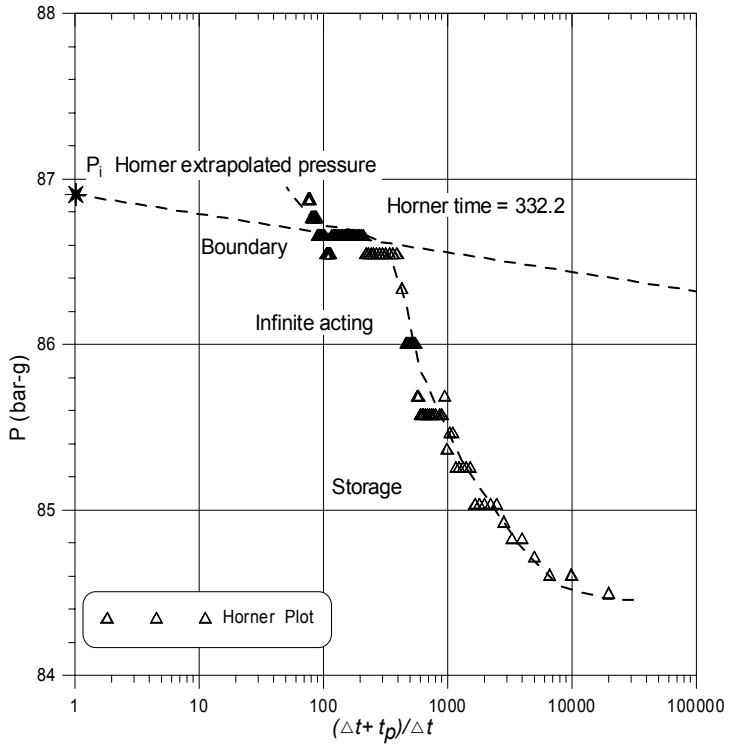

FIGURE 22: Horner plot of pressure recovery in HE-5

To obtain the skin value, the formation storage value from the semi-log analysis during the injection was used for calculation with Horner semi-log analysis formation storage. The values are shown in Table 9.

TABLE 9: Skin factor estimation for HE-5
(based on recovery data)

Injection rate (l/s)	Formation storage, skin effect included (m/Pa)	Horner formation storage (m/Pa)	Skin
40.3	2.83×10^{-9}	6.35×10^{-13}	-4.19
55.3	7.66×10^{-9}	6.35×10^{-13}	-4.69
40.3	116×10^{-8}	6.35×10^{-13}	-7.21
21.8	27.2×10^{-8}	6.35×10^{-13}	-6.48

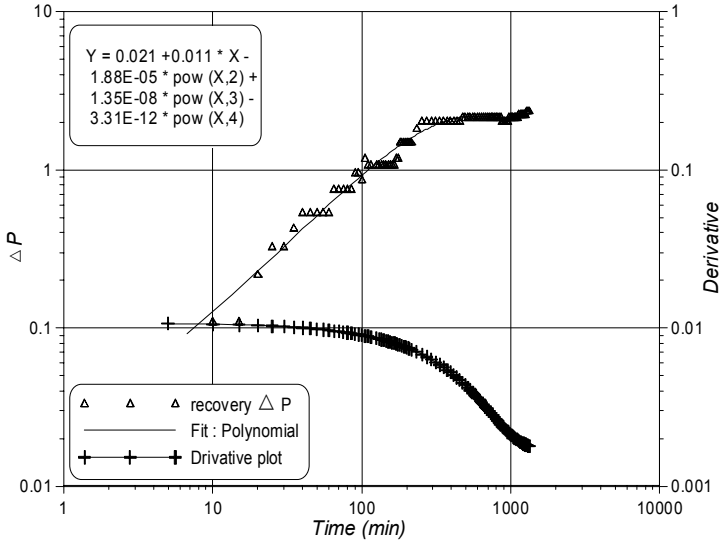

FIGURE 23: The derivative plot of the recovery data from HE-5

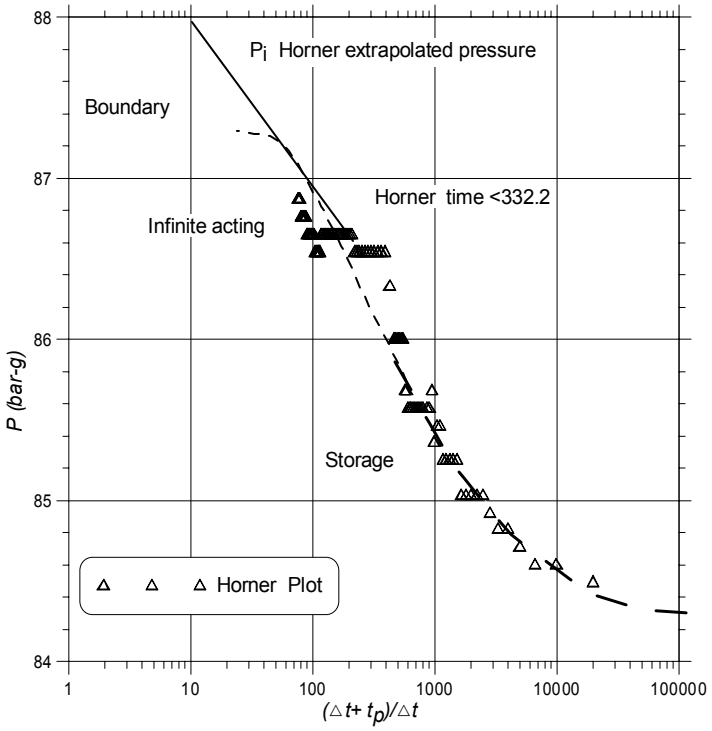

FIGURE 24: Interpretation of Horner plot data for HE-5 based on different assumptions than in Figure 22

Modern analysis has been greatly enhanced by the use of the derivative plot introduced by Horner (1995). The derivative plot provides a simultaneous presentation of log Δp vs. Δt and log $t\ dp/dt$ vs. log Δt for each data point. The advantage of the derivative plot is that it is able to display, in a single graph, many separate characteristics that would otherwise require different plots. In particular, dual porosity behaviour is much easier to see on a derivative plot, even when the first semi-log straight line is obscured by wellbore storage. Even though the derivative plot (Figure 23) is by far the most useful for diagnosis, it is not necessarily the most accurate for calculations when it comes to estimating parameters. Hence, the other plots (particularly the semi-log plots) are still required. Here, the graph illustrated in Figure 24 was approximated with a polynomial equation, and the derivative of the polynomial equation has been plotted. A Horner graph can also show the kind of boundary conditions in effect. This is, however, not demonstrated in the derivative plot (Figure 23), because there is not enough time to observe the boundary condition.

By continuing the graph shape, the effect of boundary may be seen. The reservoir's average pressure in this case is more reliable than in the first case. That value would be higher than the value in Figure 22.

5. CONCEPTUAL MODEL OF THE HELLISHEIDI AREA

Figure 25 shows the conceptual model of the Hengill area. It is based on two main assumptions, that the up-flow zone is under the central part of the Hengill volcano, and the effect of cold water is from the southern part of the area in the deeper part of the wells. The temperature reversal in the deeper part of the well supports the latter assumption in the conceptual model. Similarly, the location of the possible up-flow zone in HE-05 fits. In well HE-05, the reverse temperature effect is observed. The possible effect of the up-flow zone in this well might influence the main aquifer at 1230 m true vertical depth in the vicinity of this well, and in the upper part of the cold water.

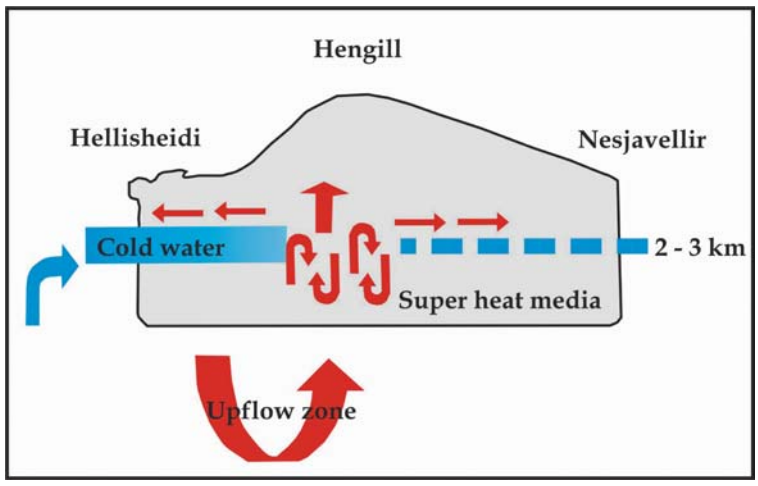

FIGURE 25: The conceptual model of Hellisheidi (modified from Björnsson and Hjartarson, 2003)

6. RESULTS AND CONCLUSIONS

- Based on analysis of injection tests and pressure recovery data, the following parameters were estimated for well HE-05. Skin value is around -6, transmissivity about 19.5×10^{-8} m^3 / Pas and formation storage of the order of 6.35×10^{-8} m / Pa.

- The warm-up, injection, and dynamic temperature profiles revealed four main feedzones located at about 763, 1119, 1230 and 1679 m true vertical depths in the well. The pressure pivot point is located at about 1230 m true vertical depth, where the main feedzone of the well is inferred to be located.

- Warm-up period data were used to estimate the formation temperature in the well. Albright method results seem to overestimate the formation temperature of the well. The Horner method estimation appears more realistic. The most reliable estimation of formation temperature is based on the last static temperature profile.

- Production test results show that the capacity of HE-05 for power generation is around 3-4 MWe, and the productivity index is 4.6 kg/s/bar.

- The wellbore simulator HOLA was used to simulate available dynamic temperature and pressure profiles. The enthalpy, simulated by HOLA is reliable. The results indicate that the productivity index for the feedzone at 1000 m true vertical depth is three times less than the index for the main zone at 1230 m true vertical depth, which correlates with the pivot point location. HOLA simulations indicate that pressure drop at the minor feed zone, up to 7 bar, does not affect the well discharge significantly. However, a five bar pressure drop at the main feed zone changes the amount of flow rate considerably.

- Based on injection test data, the injectivity index was found to be around 15.5 l/s/bar.

- The results of the analysis of data from HE-5 presented here are in an agreement with the current conceptual model of the Hellisheidi field. This includes the temperature reversal observed at depth in the well, which indicates cold inflow at deep levels from the south.

- In the pressure recovery test, boundary effects were not seen. Nevertheless, the most reliable results for formation storage and skin have been obtained through this process.

ACKNOWLEDGMENTS

I am grateful to my supervisors, Ómar Sigurdsson and Helga Tulinius, for their continuous supervision and valuable discussions during my work and to Dr. Gudni Axelsson for valuable comments to improve the report. Many thanks to Dr. Ingvar Birgir Fridleifsson, Mr. Lúdvík S. Georgsson, Mrs. Gudrún Bjarnadóttir and Mrs. Maria-Victoria Gunnarsson for their successful administration, assistance, and guidance given during the training period. I would like to thank the entire reservoir-engineering group for their keen interest in passing their skills to others.

Special thanks to the managing director of Renewable Energy Organization of IRAN, Mr. Armoodli, for accepting me as the first lady to go for this training and to work in the geothermal group. Finally, this paper is dedicated to my kind husband, Mr. Abolfazl Asghari, for the love and hope he gave me to do this work while being so far away from him.

REFERENCES

Arason, T., Björnsson, G., Axelsson, G., Bjarnason, J.Ö., and Helgason, P., 2003: *The geothermal reservoir engineering software package ICEBOX, user´s manual.* Orkustofnun, Reykjavík, report, 53 pp.

Björnsson, A., Hersir, G.P., and Björnsson, G., 1986: The Hengill high-temperature area SW-Iceland: Regional geophysical survey. *Geothermal Resources Council, Trans., 10,* 205-210.

Björnsson, G., 2002: *Using temperature and pressure logs to determine reservoir conditions and well status*. UNU-GTP, Iceland, unpublished lecture notes.

Björnsson, G., Arason, P., and Bödvarsson, G.S., 1993: *The wellbore simulator HOLA. Version 3.1. User's guide.* Orkustofnun, Reykjavík, 36 pp.

Björnsson, G., and Hjartarson, A., 2003: *Numerical model of the Hengill geothermal systems and predictions on their future status under electrical production of up to120 MWe at Hellisheidi and 120MWe at Nesjavellir.* ÍSOR, Reykjvík, report ÍSOR-2003/009 (in Icelandic), 150 pp.

Bödvarsson, G.S., Björnsson, S., Gunnarsson, Á., Gunnlaugsson, E., Sigurdsson, Ó., Stefánsson V., and Steingrímsson, B., 1990: The Nesjavellir geothermal field, Iceland. Part 1. Field characteristics and development of a three-dimensional numerical model. *J. Geotherm. Sci. and Tech., 2-3,* 189-228.

Franzson, H., and Kristjánsson, B.R., 2003: *Geological settings at the Hellisheidi production field.* ÍSOR, report HF/BRK-2003-02 (in Icelandic), 22 pp.

Gudmundsson, Á., Richter, B., Franzson, H., Thordarson, S., Hermannsson, G., Daníelsson, P.E., Sigurdsson, Ó., and Gudnason, Ó., 2002: *Hellisheidi, well HE-05, 3rd phase: Drilling of production part from 802 to 2000 m depth.* Orkustofnun, Reykjavík, report OS-2002/026 (in Icelandic), 84 pp.

Gunnlaugsson, E., 2003: Reykjavík Energy - District heating in Reykjavík and electrical production using geothermal energy. In: Fridleifsson, I.B., and Gunnarsson, M.V. (eds.), *Lectures on sustainable use and operating policy for geothermal resources.* Short course prior to the International Conference IGC2003 on "Multiple Integrated Use of Geothermal Resources", UNU-GTP, Iceland, publ. 1, 67-78.

Hersir, G.P., Björnsson, G., Björnsson, A., 1990: *Volcanoes and geothermal systems in the Hengil area, Geophysical exploration*. Orkustofnun, Reykjavik, report OS-90031/JHD-06 (in Icelandic), 92 pp.

Hjartarson, A., 2002: *Pressure transient analysis (well testing theory)*. UNU-GTP, Iceland, unpublished lecture notes.

Horne, R.N., 1995: *Modern well test analysis, a computer aided approach* (2nd edition). Petroway Inc., USA, 65-77.

James, R., 1970: Factors controlling borehole performance. *Geothermics, Sp. issue, 2-2,* 1502-1515.

Jónsson, S., Gudmundsson, Á., Hermannsson, G., Sigurdsson, Ó., Gudlaugsson, S., and Skarphédinsson, T., 2002: *Well HE-05 at Hellisheidi. Siting and design of the well.* Orkustofnun, Reykjavík, report OS-2002/024 (in Icelandic), 5 pp.

Saemundsson, K., Snorrason, S.P., and Fridleifsson, G.Ó., 1990: *Geological map of the southern Hengill area, between Hengladalir and Krossfjöll*. Orkustofnun, Reykjavík, report OS-90008/JHD-02 B (in Icelandic), 15 pp.

Stefánsson, V., and Steingrímsson, B.S., 1990: *Geothermal logging I, an introduction to techniques and interpretation* (3rd edition). Orkustofnun, Reykjavík, report OS-80017/JHD-09, 117 pp.

Steingrímsson, B., 2003: *Discharge measurements and injection tests*. UNU-GTP, Iceland, unpublished lecture notes.